

## Silica Monoliths Templated on L<sub>3</sub> Liquid Crystal

Abds-Sami Malik,<sup>†,‡</sup> Daniel M. Dabbs,<sup>†</sup> Howard E. Katz,<sup>§,||</sup> and Ilhan A. Aksay<sup>\*,†</sup>

Department of Chemical Engineering, Princeton University, Princeton, New Jersey 08544, and Bell Laboratories, Lucent Technologies, Murray Hill, New Jersey 08904

Received June 3, 2005. In Final Form: October 13, 2005

Dimensionally stable, optically clear, highly porous (~65% of the apparent volume), and high surface area (up to 1400 m<sup>2</sup>/g) silica monoliths were fabricated as thick disks (0.5 cm) by templating the isotropic liquid crystalline L<sub>3</sub> phase with silica through the hydrolysis and condensation of a silicon alkoxide and then removing the organic constituents by supercritical ethanol extraction. The L<sub>3</sub> liquid crystal is a stable phase formed by the cosurfactants cetylpyridinium chloride monohydrate and hexanol in HCl(aq) solvent. Extracted 0.5 cm thick disks exhibited a low ratio of scattered to transmitted visible light ( $1.5 \times 10^{-6}$  at 22° from the surface normal). The degree of silica condensation in the monoliths was high, as determined by <sup>29</sup>Si NMR measurements of Q<sub>3</sub> and Q<sub>4</sub> peak intensities (0.53 and 0.47, respectively). As a result, the extracted and dried monoliths were mechanically robust and did not fracture when infiltrated by organic solvents. Photoactive liquid monomers were infiltrated into extracted silica monoliths and polymerized in situ, demonstrating the possible application of templated silica to optical storage technology.

### Introduction

Photopolymer composites typically consist of a photoactive component held within the interstitial volumes and channels of a matrix.<sup>1</sup> A two-photon process, combining a modulated signal beam with a reference beam within a photopolymer composite, can be used to write a holographic optical pattern, or grating, through preferential photoreaction by the monomer.<sup>2</sup> The grating has both spatial and angular dependence, and the original pattern can be recovered by reading the grating with a reference beam held at the same angle. Several such gratings can then be written to the same spatial volume, separated from each other by the Bragg effect.<sup>3</sup> These composites are of interest for use in optical storage applications, but developments have been hampered by the lack of a suitable host matrix.<sup>4,5</sup> The utility of the composite depends on the physical properties of the host, including rigidity, environmental stability, and thickness. The optical properties of the matrix, such as its transparency to visible wavelengths, affect the optical properties of the composite.<sup>2,6</sup> The composites must exhibit high dimensional stability to avoid degraded or lost data caused by shape changes in the matrix that could affect the spatial and angular location.

Suggested photopolymer composites include binary photopolymer systems,<sup>7,8</sup> organic–inorganic nanocomposites,<sup>9,10</sup> and photomonomers either infiltrated into porous glass<sup>11</sup> or mixed

with sol–gel precursors<sup>6</sup> to form porous photoactive glasses. In general, each of these systems suffers from limitations in the respective processing and/or structural properties.<sup>4,5</sup> Binary photopolymer systems offer high chemical compatibility between matrix and photomonomers but exhibit poor transparency to visible wavelengths.<sup>6,11</sup> The low transmissivity of the photopolymer<sup>12</sup> limits the form of the composite: thin films must be used to ensure adequate transmission of light. This limitation to the physical volume reduces the space available for storing data. Additionally, polymer matrixes are not physically robust and can warp and distort, exhibiting significant changes in volume and flexibility with changes in environment or under illumination.<sup>6,11</sup> Vycor, a nanoporous silica glass, has been shown to be a dimensionally stable matrix for photomonomers, combining excellent optical properties with increased thickness.<sup>11</sup> But channel access is poor in Vycor, demonstrated by the several days to weeks required for complete infiltration by a liquid. The effective void volume in the matrix is low, limiting the amount of photomonomer that can be held in the matrix.<sup>11,13</sup> Photoactive glasses from sol–gels<sup>6</sup> have been made that exhibit high diffraction efficiency (near 100%) coupled with excellent dimensional stability, but sol–gel processing requires careful matching among the chemistries of the sol–gel precursor(s), photoinitiator, and photomonomer to ensure uniform distribution of the photoactive material throughout the silica matrix.

Thick, optically transparent matrixes with high void volume suggest the use of silica aerogels, obtained by supercritical CO<sub>2</sub> extraction of silica sol–gels.<sup>14</sup> But the very high porosity in aerogels contributes to the fragility of these materials, making them difficult to manipulate.<sup>15,16</sup> Infiltrating an aerogel with a liquid must be done very slowly to avoid high stress gradients created by differential capillary pressures building up within the matrix as the liquid penetrates the channels of the aerogel, which

\* Corresponding author. E-mail: iaksay@princeton.edu.

<sup>†</sup> Princeton University.

<sup>‡</sup> Currently at Diamond Innovations, Worthington, OH 43085.

<sup>§</sup> Lucent Technologies.

<sup>||</sup> Currently at Johns Hopkins University, Baltimore, MD 21218.

(1) Liu, G.-D.; He, Q.-S.; Luo, S.-J.; Wu, M.-X.; Jin, G.-F.; Shi, M.-Q.; Wu, F.-P. *Chin. Phys. Lett.* **2003**, *20*, 1733–5.

(2) Psaltis, D.; Mok, F. *Sci. Am.* **1995**, *273*, 70–76.

(3) Coufal, H. *Nature* **1998**, *393*, 628–9.

(4) Haw, M. *Nature* **2003**, *422*, 556–8.

(5) Suzuki, N.; Tomita, Y.; Kojima, T. *Appl. Phys. Lett.* **2002**, *81*, 4121–3.

(6) Cheben, P.; Calvo, M. L. *Appl. Phys. Lett.* **2001**, *78*, 1490–2.

(7) Schilling, M. L.; Colvin, V. L.; Dhar, L.; Harris, A. L.; Schilling, F. C.; Katz, H. E.; Wysocki, T.; Hale, A.; Blyler, L. L.; Boyd, C. *Chem. Mater.* **1999**, *11*, 247–54.

(8) Karpov, G. M.; Obukhovskiy, V. V.; Smirnova, T. N.; Lemesheko, V. V. *Opt. Commun.* **2000**, *174*, 391.

(9) Levy, D.; Esquivias, L. *Adv. Mater.* **1995**, *7*, 120–9.

(10) Beecroft, L. L.; Ober, C. K. *Chem. Mater.* **1997**, *9*, 1302–17.

(11) Schnoes, M. G.; Dhar, L.; Schilling, M. L.; Patel, S. S.; Wiltzius, P. *Opt. Lett.* **1999**, *24*, 658–60.

(12) Emslie, C. *J. Mater. Sci.* **1988**, *23*, 2281–93.

(13) Vichit-Vadakan, W.; Scherer, G. W. *J. Am. Ceram. Soc.* **2000**, *83*, 2240–5.

(14) Brinker, C. J.; Scherer, G. W. *Sol–Gel Science: The Physics and Chemistry of Sol–Gel Processing*; Academic Press: New York, 1990.

(15) Novak, B. M.; Auerback, D.; Verrier, C. *Chem. Mater.* **1994**, *6*, 282–6.

(16) Leventis, N.; Sotiriou-Leventis, C.; Zhang, G. H.; Rawashdeh, A. M. M. *Nano Lett.* **2002**, *2*, 957–60.

can ultimately lead to the mechanical failure of the silica framework.<sup>17</sup>

In this paper we describe the fabrication of dimensionally stable, optically clear silica monoliths with high void volumes (~65 vol %). Our method uses supercritical ethanol extraction of the surfactants from an L<sub>3</sub> liquid crystal templated with silica to fashion porous silica that resembles aerogels in void volume and channel accessibility but combined with physical and optical properties more similar to those of Vycor glass. We show that, due to the uniform distribution of the void space and uniform wall thickness, the matrix is strong enough to withstand infiltration by monomeric liquids and in situ polymerization of photoactive monomers, suggesting that this material would be a promising candidate for applications in optical storage.

We have previously described the processing of porous silica formed by the templation of the isotropic L<sub>3</sub> liquid crystalline phase.<sup>18,19</sup> Our goal in this past work was to fabricate mesoporous structures with randomly oriented, isotropic channels of uniform channel diameter. A channel network based on the L<sub>3</sub> crystal template would have large continuous channels (20–100 nm diameter) that extend throughout the monolith. The L<sub>3</sub> liquid crystal phase is a thermodynamically stable phase formed by mixing the cosurfactants cetylpyridinium chloride monohydrate (CpCl·H<sub>2</sub>O) and hexanol in aqueous solutions of NaCl<sup>20</sup> or HCl.<sup>18,19</sup> The structure of the liquid crystal is simply described as an isotropic three-dimensionally interconnected network of uniform channels with tunable diameter, the open channels defined by surfactant bilayer walls and filled only by the aqueous solvent.<sup>18–23</sup> The channel structure was replicated in silica using the surfactant bilayer walls as the template for condensing hydrolyzed tetramethoxysilane (TMOS).<sup>18,19</sup> Monoliths formed by L<sub>3</sub> templation retained structure while under solvent, were optically clear, and were shown to preserve the liquid crystal's nonperiodic channel network and uniform channel size distribution.<sup>18,19</sup> However, drying usually resulted in fragmentation, typically forming powders or granules. Slow, carefully controlled drying yielded larger pieces, but these were invariably cracked and suffered from significant shrinkage (up to 50% of the initial volume).<sup>18,19</sup>

Discoloration, shrinking, and cracking during subsequent heat treatments were found to be serious disadvantages with as-dried L<sub>3</sub> silica. In an effort to improve the mechanical and optical properties, combinations of extractions and heat treatments were tried. Supercritical CO<sub>2</sub> extraction proved to be ineffective in removing the organic template and byproducts of the hydrolysis and condensation of the silicon alkoxide. Heat treating monoliths also failed, resulting in samples that were heavily cracked at best and usually fragmented and that appeared cloudy or discolored.<sup>19,24</sup> Cloudiness, especially in CO<sub>2</sub>-extracted samples, resulted from retained water, and discoloration was caused by organic residue—the solubility of the polar CpCl·H<sub>2</sub>O surfactant is not high in CO<sub>2</sub>.<sup>19,24,25</sup> Heating the silica to higher temperatures

and/or for longer times appeared to cause the loss of channels through densification of the monolith.

Continuous solvent (Soxhlet) extraction proved effective in obtaining environmentally stable, intact monoliths, but this process failed to completely remove the organic materials.<sup>24</sup> When compared to preliminary supercritical extraction experiments using methanol as the extracting solvent, solvothermal extraction was not as effective in increasing void volumes and surface areas.<sup>24</sup> Heat treating solvothermally extracted samples often resulted in coloration, not as severe as that seen in the unextracted or CO<sub>2</sub>-extracted silica, but sufficient to reduce the transmission of visible wavelengths. Samples were strong enough to withstand liquid infiltration, most likely because continuous solvent extraction kept the monolith at higher temperatures under solvent for long periods (up to 4 days) and thus yielded stronger cell walls due to polymerization.

The procedure we describe here improves upon our past efforts by almost completely removing the organic component from the templated silica, maintaining high optical quality during subsequent heat treatments, and strengthening the monolith to withstand subsequent liquid infiltration and polymerization. The resulting optical properties of trial photopolymer composites are excellent.

## Experimental Section

**Templation of the L<sub>3</sub> Phase.** We have previously described in detail the procedure for templating silica onto the L<sub>3</sub> liquid crystalline phase<sup>19</sup> and so provide only a brief outline of the process here. The L<sub>3</sub> phase was formed by mixing the cosurfactants cetylpyridinium chloride monohydrate (CpCl·H<sub>2</sub>O) and hexanol in 0.2 M HCl(aq) solvent. TMOS was the chosen templating agent. All compounds were obtained from Aldrich Chemical (Milwaukee, WI) and used as received, excepting the HCl(aq), which was diluted with triply distilled water to 0.2 M. Hexanol (0.45 g) and CpCl·H<sub>2</sub>O (0.40 g) were first gently mixed to form a homogeneous paste. The 0.2 M HCl (1.0 g) solvent was added to the paste and the mixture stirred vigorously until the solution became clear (20–30 min). This vigorous stirring is essential for the conversion of CpCl·H<sub>2</sub>O from lamellar (its as-received form) to the L<sub>3</sub> structure.<sup>26</sup> Solutions that did not clear within 30 min were discarded. The apparent viscosity of the final solution was similar to that of water. The solution was silicified by slowly adding TMOS (2.0 g). The hydrolysis of TMOS in acid solution is very exothermic so TMOS was added dropwise to the stirred solution to avoid overheating.

After cooling, the liquid solution was cast into 2.5 cm diameter plastic Petri dishes to a depth of 1 cm, tightly sealed and placed in an airtight container to prevent drying. Left undisturbed at room temperature, a typical solution gelled within 2–3 days to form a clear solid monolith. Gelation was considered complete when the monolith no longer flowed when tilted.

To reduce the possibility of cracking when the monolith was exposed to solvent changes, it was necessary to perform a series of solvent exchanges, systematically replacing the initial solvent with pure methanol, a liquid with surface tension lower than that of water, to reduce the capillary pressures associated with drying.<sup>27</sup> The first solvent exchange was done using a methanol/water solution (~40 mL, 50% each by volume), closely matching the polarity and composition of the liquid solution filling the channels of the gel following the hydrolysis and condensation of TMOS. This step was necessary to avoid solvent gradients within the gel leading to differential stresses in the gel body.<sup>28,29</sup> After 1 day this initial wash

(17) Merzbacher, C. I.; Barker, J. G.; Swider, K. E.; Rolison, D. R. *J. Non-Cryst. Solids* **1998**, *224*, 92–6.

(18) McGrath, K. M.; Dabbs, D. M.; Yao, N.; Aksay, I. A.; Gruner, S. M. *Science* **1997**, *277*, 552–6; **1998**, *279*, 1289.

(19) McGrath, K. M.; Dabbs, D. M.; Yao, N.; Edler, K. J.; Aksay, I. A.; Gruner, S. M. *Langmuir* **2000**, *16*, 398–406.

(20) McGrath, K. M. *Langmuir* **1997**, *13*, 1987–95.

(21) Schwarz, B.; Mönch, G.; Ilgenfritz, G.; Strey, R. *Langmuir* **2000**, *16*, 8643–52.

(22) Carlsson, I.; Wennerström, H. *Langmuir* **1999**, *15*, 1966–72.

(23) Roux, D.; Coulon, C.; Cates, M. E. *J. Phys. Chem.* **1992**, *96*, 4174–87.

(24) Dabbs, D. M.; Mulders, N.; Aksay, I. A. Solvothermal Removal of the Organic Template from L<sub>3</sub> Templated Silica Monoliths. Submitted for publication in *J. Nanoparticle Res.*

(25) McHardy, J.; Sawan, S. P., Eds. *Supercritical Fluid Cleaning: Fundamentals, Technology, and Applications*; Noyes Publications: Westwood, NJ, 1998.

(26) Bhansali, S. H.; Malik, A.-S.; Jarvis, J. M.; Akartuna, I.; Dabbs, D. M.; Carbeck, J. D.; Aksay, I. A. The Stability of L<sub>3</sub> Sponge Phase in Acidic Solutions. Submitted for publication in *Langmuir*.

(27) Hensch, L. L.; West, J. K. *Chem. Rev.* **1990**, *90*, 33–72.

(28) Barati, A.; Kokabi, M.; Famili, M. H. N. *J. Eur. Ceram. Soc.* **2003**, *23*, 2265–72.

(29) Harrel, J. H.; Ebina, T.; Tsubo, N.; Stucky, G. *J. Non-Cryst. Solids* **2002**, *298*, 241–51.

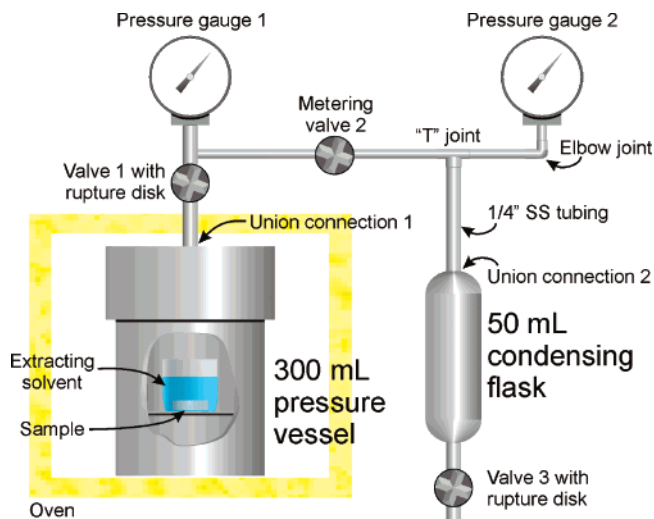


**Figure 1.** Schematic diagram of supercritical drying apparatus. The 300 mL pressure vessel was loaded with sample under ethanol and placed into a high-temperature oven (shaded square). The rest of the equipment was kept out of the oven.

was replaced by a solution of 75/25 methanol/water, and after another day, with methanol. The methanol wash was repeated 2–3 times. It was assumed that all water and accessible organic had been removed from the gel when no residue was apparent in the evaporated methanol wash. During solvent exchange a typical disk shrank by less than <5% across its diameter, enough to permit easy removal from the Petri dish. The resulting disks were clear and free of cracks, physically fragile, and would fracture if dried in air. Solvent exchanges with ethanol were done in like manner for samples that were to be supercritically extracted.

**Supercritical Extraction.** Ethanol was chosen as the supercritical extraction solvent for several reasons: (i) the respective solubilities of the cosurfactants  $\text{CpCl}\cdot\text{H}_2\text{O}$  and hexanol in either ethanol or methanol are very similar;<sup>24</sup> (ii) ethanol and its extraction byproducts are less noxious; and (iii) ethanol has a comparatively moderate critical temperature (240 °C) and pressure (6.12 MPa).

A schematic for the supercritical drying apparatus is shown in Figure 1. The components were obtained from Parr Instruments (Moline, IL), Swagelok (Solon, OH), and High Pressure Equipment Co. (Erie, PA). A 300 mL 316 alloy stainless steel pressure vessel (Parr No. 4761) equipped with a pressure gauge and valve with 20.68 MPa rupture disk (Parr gauge block assembly #NJ4316PDA) was used as the extraction chamber. A Teflon gasket was sufficient to form the seal between the cap and chamber. This unit was connected by 316 stainless steel alloy 6.35 mm ( $1/4$  in.) tubing (Swagelok No. 457HC2) to a Grafoil packed metering valve (Swagelok No. SS-31RS4-G-3263) to permit the controlled release of supercritical fluid into a 50 mL 316 stainless steel alloy pressure vessel (Swagelok No. 304L-HDF4–50). A second pressure gauge (High Pressure No. 4PG5) was used to monitor the pressure in the second pressure vessel during the release of pressure from the extraction chamber.

The gel monolith was loaded into the 300 mL pressure vessel along with ~210 mL of ethanol and sealed following the manufacturer's instructions. The chamber was placed in an oven and connected via stainless steel tubing to the 50 mL condensing flask (Figure 1). The chamber was slowly heated at a rate of 0.2 °C/min. to 230 °C and held at this temperature for 60–90 min to allow the vessel to equilibrate. The temperature was then raised to 260 °C at a rate of 0.1 °C/min. The pressure climbed rapidly to 10 MPa during this heating step. The sample was equilibrated at 260 °C for 3–4 h. [Valve 1 was briefly opened as needed during temperature ramping and isothermal soak to keep the chamber pressure below 10 MPa.]

The rate of depressurization was kept slow to lessen stress on the sample by preventing large pressure differences between the sample interior and the chamber atmosphere. A cycle started by opening valve 1 while keeping valve 2 closed and holding the chamber

temperature at 260 °C. The pressure was reduced in ~0.5 MPa increments by opening and closing valve 2. After each stepwise reduction, the system was held at pressure for 30–60 min to equilibrate. Stepped reductions were repeated until the values on gauges 1 and 2 were equal (15–20 steps). Valve 2 was then closed and valve 3 opened to remove the condensate from the condensing flask. [Adequate ventilation of the extraction apparatus was required to avoid exposure to the extraction byproducts.] Valve 3 was closed, and the entire cycle was repeated until all of the supercritical ethanol had been removed from the chamber (typically 4 complete cycles).

After the chamber pressure equaled the ambient pressure, the chamber, still at 260 °C, was evacuated under dynamic vacuum, by connecting a vacuum line to the condensing chamber and opening valves 2 and 3. After ~8 h, the sample was oven-cooled to 50 °C (~6 h) and kept under vacuum for another 48 h to anneal.

**Characterization of the Silica Monoliths.** Thermogravimetric analysis (TGA) was performed in air on a Perkin-Elmer (Wellesley, MA) Pyris instrument, and nitrogen adsorption isotherms were acquired using a Micromeritics (Norcross, GA) ASAP 2010. Transmission FTIR spectroscopy was performed on powders suspended in pressed KBr pellets using a Thermo-Nicolet (Madison, WI) Magna-IR 560 FT-infrared spectrophotometer. Elemental analysis for C, H, and N was done by Robertson Microлит Laboratories, Inc. (Madison, NJ). Void volume was determined by helium pycnometry using a Micromeritics AccuPyc system and confirmed by measuring the dielectric constants of representative monoliths using a capacitance/loss bridge (Andeen Hagerling Model 2500A, Cleveland, OH). Capacitors were prepared by evaporating gold layers on both sides of 1.9 mm thick silica sample disks and heating the samples above 100 °C to remove moisture.

Solid-state  $^{29}\text{Si}$  NMR spectra, recorded on a Varian (Palo Alto, CA) 400 MHz NMR spectrometer at 79 MHz with magic angle spinning and proton decoupling, was used to quantify the degree of condensation within the silica network.<sup>30</sup> The delay between pulses was set to 100 s, and a small flip angle pulse was used to obtain quantitative spectra.

**Infiltration with a Liquid and in Situ Polymerization.** Extracted and dried monoliths were prepared for infiltration with liquid by exposing the sample to ethanol vapor at room temperature. After 12–24 h exposure, monoliths could be submerged in liquid ethanol without cracking. Other liquids, such as hexane, xylene, silicone oil, hydroxyethyl acrylate, and isobornyl acrylate, could be introduced after vapor saturation. The two acrylates were chosen because both are photopolymerizable monomers of interest for optoelectronic applications. In this study, a mixture of hydroxyethyl acrylate and photoinitiator [bis(eta-5–2,4-cyclopentadien-1-yl)bis(2,6-difluoro-3-(1*H*-pyrrolyl) phenyltitanium (Ciba-Geigy 784, Basel, Switzerland)] was infiltrated into a silica monolith and polymerized by flood exposure under a UV lamp.<sup>7</sup> FTIR spectroscopy was used to confirm the extent of polymerization.

## Results and Discussion

A successfully extracted and annealed sample is shown in Figure 2. The monolith has the shape of its gelling mold (a Petri dish), is transparent to visible light, colorless, and has no obvious flaws. These materials can be handled without special precautions, and subsequent heat treatments up 600 °C do not cause cracking, discoloration, or shape changes. After vapor saturation with ethanol, the monolith can withstand reinfiltration by liquid and in situ polymerization of monomer infiltrants. Composite coloration and transparency depend on the nature of the polymer and polymerization reagents. In the polyacrylates used here, the resulting composites were initially colored due to the presence of photoinitiator, but the intensity of the color faded over time and the final composite closely resembled the uninfiltrated matrix shown in Figure 2.

(30) Grimmer, A. R.; Rosenberger, H.; Bürger, H.; Vogel, W. *J. Non-Cryst. Solids* **1988**, *99*, 371–8.

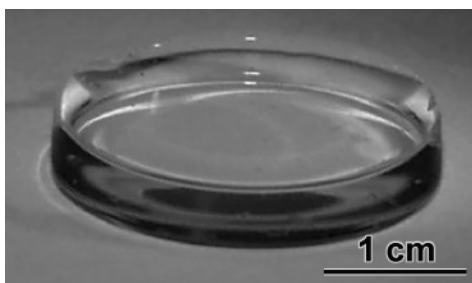


**Figure 2.** Representative silica sample following supercritical ethanol extraction. The original gel was cast into the shape of a disk using a Petri dish. The rim at the edge of the disk formed through the wetting of the dish by the liquid silica solution before gelling.

**Supercritical Extraction.** The entire process needed to produce a good sample took between 4 and 7 days, from loading the sample gel into the extraction chamber to removing the extracted monolith. Most of the required time was needed to slowly depressurize the chamber following extraction plus that required for annealing under vacuum. Extraction was assumed complete at the end of the depressurization cycle when the pressure in the extraction chamber (Figure 1) matched the ambient pressure, the point at which fluid would no longer flow spontaneously from the extraction chamber into the condensing chamber. Depressurization took 1–2 days, depending on the initial amounts of solvent and extractant in the chamber, the time allowed for each stepwise reduction in pressure, and the time allowed for equilibration following a pressure reduction step. To ensure complete removal of solvent and to anneal the matrix, the sample was kept under dynamic vacuum and heated for 2–3 days while still in the extraction chamber.

The construction of the extraction system made it impossible to determine the state of the sample after loading and before removing it from the chamber. As noted in the described procedure, the pressure in the extracting chamber was monitored at all times. The pressure in the sample chamber was periodically reduced by slightly opening valve 1 (Figure 1) during extraction to relieve excess pressure. If during this procedure the pressure was allowed to fall below the critical point, the sample could fracture due to the high capillary pressures that would form in the monolith. Also, during the depressurization step at the end of the extraction process, it was necessary to reduce the pressure slowly over a long period to allow ample time for the monolith to equilibrate with the ambient environment. Too-rapid depressurization would prevent any remaining fluid from escaping the monolith, and capillary pressures could rise to damaging levels. The overall yield of unbroken monoliths against the total number of attempts approached 50% with practice.

**Extraction Efficiency.** In our earlier work on  $L_3$  silica matrixes, discoloration and reduction in the transparency to visible light were determined to be due to the presence of organic residue after heat treatments and inadequate solvent extractions.<sup>18,24</sup> Thermogravimetric analysis (Figure 3) was used to compare the efficiency of extraction for samples extracted using supercritical  $CO_2$  to that for samples extracted using supercritical ethanol. The degradation profile for the  $CO_2$  extracted sample resembles that of unextracted  $L_3$  silica<sup>24</sup> with slightly less total weight loss. The more significant weight loss below 250 °C exhibited by the  $CO_2$ -extracted sample and the pronounced inflection in the curve near 200 °C implies that supercritical carbon dioxide was at least partially effective in removing organics, most likely the less-polar hexanol cosurfactant. It was less effective in removing the solvent retained in the channels of the silica, signified by the large weight loss below 250 °C. Prior to  $CO_2$  extraction, the

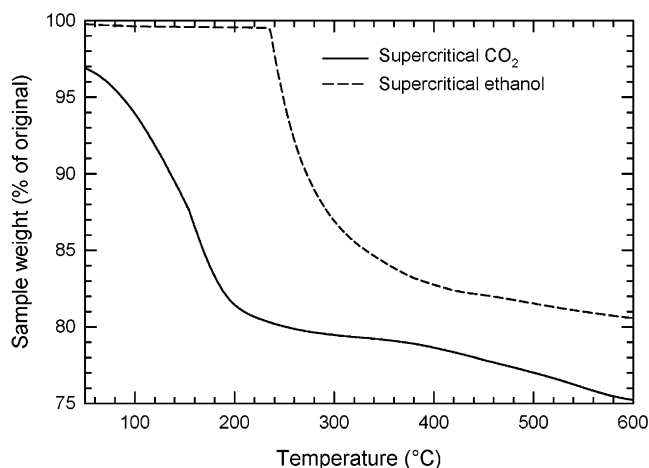


**Figure 3.** Typical TGA traces for surfactant-templated silica samples dried in supercritical carbon dioxide and supercritical ethanol. Silica that was dried using supercritical ethanol showed much better thermal stability up to almost 250 °C. After 250 °C, the weight loss was attributed to adsorbed water or alcohol on the silica surface. For silica dried in supercritical carbon dioxide there was a nearly constant weight loss above 250 °C, which was attributed to the loss of organic surfactant from the silica. Thus it was surmised that supercritical ethanol processing was much better at removing organic components from the silica.

sample was solvent-exchanged with methanol. The retention of this solvent during  $CO_2$  extraction most probably explains the weight loss below 250 °C. The degradation of the  $CpCl \cdot H_2O$  surfactant entrapped in the silica walls is a reasonable explanation for the long “tail” seen in the thermal profile above 250 °C, matching previous observations.<sup>19,24</sup>

In contrast, there is little weight loss up to almost 250 °C in samples that underwent extraction by supercritical ethanol, indicating little retention of solvent within the channels or surfactant in the channel walls. In a companion study, we showed that a solvothermally extracted sample exhibited a similar weight loss profile albeit with a much more abrupt, stepwise appearance, and differential scanning calorimetry results indicated that organics were retained by the extracted samples.<sup>24</sup> With supercritically extracted samples, weight loss above 250 °C does not appear to be due to retained  $CpCl \cdot H_2O$  surfactant. As confirmation, elemental analysis of supercritically extracted samples could not detect C, H, or N in the monoliths. Also, supercritical ethanol-extracted samples did not discolor during high-temperature heat treatments (up to 600 °C), whereas solvothermally extracted samples were typically colored following heat treatment. While the amount of total weight loss is comparable between solvothermal and ethanol-extracted samples, ~18% total weight loss,<sup>24</sup> the mechanisms for the respective thermal profiles above 250 °C are different. In the case of the solvothermally extracted samples, approximately 3% of the original sample weight is lost below 100 °C, indicating the retention of some volatile material. This is followed by a sharp decrease in weight beginning at ~250 °C, similar to that observed in the supercritical ethanol-extracted samples described in this study. But the supercritically extracted samples are very dry, exhibiting only insignificant weight loss prior to 250 °C (Figure 3). Due to the (slight) coloration seen in solvothermally extracted samples that have been heat-treated following extraction, we suspect that some of the retained solvent in these materials is organic.

The supercritically extracted  $L_3$  silica is likely to be very hygroscopic, similar to aerogels prior to heat treatment,<sup>14</sup> in contrast to the solvothermally extracted samples which appear to retain some of the extracting solvent after the Soxhlet process.<sup>24</sup>

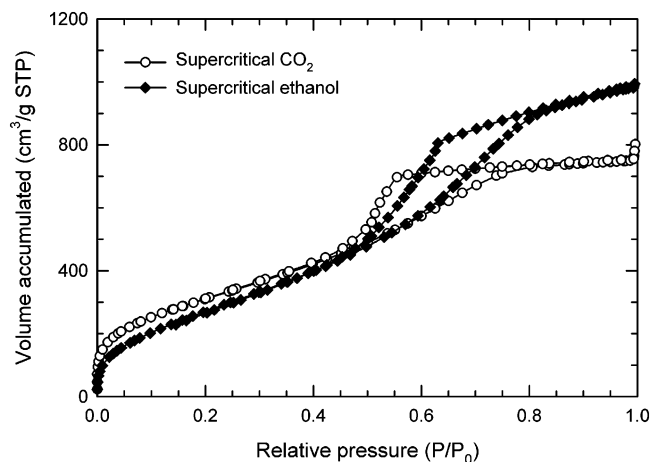


**Figure 4.** Typical nitrogen mass accumulation isotherms for surfactant-templated silica samples dried in supercritical carbon dioxide or supercritical ethanol. At low relative nitrogen pressures, the two samples are similar; however, at higher relative pressure ( $>0.6$ ) the sample that was dried in supercritical ethanol exhibits more nitrogen accumulation, corresponding to a larger cumulative void volume. The calculated surface areas (using the BET model) ranged from 1000 to 1400  $\text{m}^2/\text{g}$ . The void volumes ranged from 50 to 65% total volume.

The adsorption of water from the environment may well explain the nature of the weight loss at temperatures above 250 °C for the supercritically extracted samples, the results of elemental analysis, and the high optical clarity of these samples following high-temperature heat treatments. It also suggests that these materials must be protected from exposure to water vapor prior to heat treatment.

**$L_3$  Silica following Supercritical Extraction.** High void volume in the matrix is a necessary property for photopolymer composites, needed to maximize the amount of the photoactive component in the composite and increase, in the case of storage media, the data storage capacity. Nitrogen “accumulation” measurements were used to determine the void volume and effective surface area of extracted monoliths (Figure 4). The isotherms that result from these measurements are commonly referred to in the literature as “nitrogen adsorption” isotherms. Since the isotherm shows evidence of adsorption as well as condensation of liquid in the channels, referring to the entire isotherm as an “adsorption isotherm” is not accurate and hence we refer to these isotherms as accumulation isotherms. We determine the surface areas of the supercritically extracted gels by applying the BET model to the region of the isotherm that results from multilayer adsorption.<sup>31</sup>

In the isotherms shown in Figure 4, nitrogen accumulates via monolayer–multilayer adsorption up to  $\sim 0.5 P/P_0$ . For both the accumulation isotherms— $L_3$  silica dried in supercritical  $\text{CO}_2$  and supercritical ethanol—this region of the isotherm overlaps, indicating that the two extraction solvents result in gels with similar surface areas. The calculated BET surface areas of  $L_3$  silica ranged between 1000 and 1400  $\text{m}^2/\text{g}$ , in close agreement to our preliminary studies using supercritical methanol extraction<sup>24</sup> and comparable to silica aerogels.<sup>14</sup>

For relative pressures beyond  $0.5 P/P_0$ , the respective isotherms for the  $L_3$  silica supercritically dried in the two solvents begin to differ. The volume of nitrogen accumulated is greater in the monoliths supercritically dried in ethanol than in those supercritically dried in  $\text{CO}_2$ , as seen by the capillary condensation

regions of the two isotherms. The void volume in the supercritically extracted monoliths was determined to range from 1.0 to 1.2  $\text{cm}^3/\text{g}$ , from the isotherms (Figure 4)<sup>31–33</sup> and from helium pycnometry measurements. The larger volumes resulting from  $L_3$  silica gels dried supercritically in ethanol, with surface areas similar to that of gels dried in supercritical  $\text{CO}_2$ , suggests that supercritical ethanol is a better solvent for effectively drying these gels without loss of porosity. Bulk volumes were between 1.6 and 1.8  $\text{cm}^3/\text{g}$ , so 60–65% of the  $L_3$  silica volume was void, significantly higher than that found in Vycor 7930 porous glass<sup>34</sup> and within the range of silica aerogels.<sup>14</sup>

Another check on the measured value of the void volume is through the comparison of the dielectric constant of the matrix material, silica, and the measured constant of a simple capacitor made by gold-coating opposite sides of an  $L_3$  monolith and heating the sample to 100 °C to remove moisture. The dielectric constant, as measured under ambient conditions, was 1.6 for the supercritically extracted  $L_3$  silica monoliths. Then, assuming that the walls of the material are composed of fused silica having a dielectric constant of 4.1 (1 MHz, 20 °C)<sup>35,36</sup> and the remainder of the volume is composed of air, this value corresponds to a void volume between 50% total volume (in the series limit) and 80% total volume (in the parallel limit). For comparison, Vycor 7930 has a void volume of 28% of the total volume and a dielectric constant of 3.1 at 25 °C and 100 Hz.<sup>34</sup>

The calculated dielectric constant assumes that the material consists entirely of dry silica and air. It is possible that water was adsorbed onto the pore surfaces when the measurement was taken. If this had been the case, then we would conclude that the pore fraction is even higher, since the dielectric constant of the water adlayer would presumably be even higher than that of the silica, and an even greater volume fraction of air would have had to be present to produce the greatly diminished dielectric constant observed.

Strength in a silica matrix is related to the degree of condensation within the silicon oxide network, higher condensation implying more cross-linking between silicon centers through oxygen bridges.<sup>14</sup> A standard method for determining the extent of condensation in a silica framework is  $^{29}\text{Si}$  NMR, comparing the relative intensities of the  $Q_1$ ,  $Q_2$ ,  $Q_3$ , and  $Q_4$  peaks (chemical shifts between  $-85$  and  $-110$ ).<sup>30</sup> In supercritical ethanol-extracted  $L_3$  silica the  $Q_3$  and  $Q_4$  peaks were very intense, measuring 0.53 and 0.47, respectively, indicating a high degree of condensation within the silica framework.  $Q_2$  peak intensities were very small to nonexistent. The  $^{29}\text{Si}$  NMR spectrum of  $\text{CO}_2$ -extracted  $L_3$  silica was very different: the relative intensities of the  $Q_2$ ,  $Q_3$ , and  $Q_4$  peaks were 0.16, 0.57, and 0.27, respectively, indicating much less condensation within the silica matrix. A simple explanation is the difference in critical temperatures, 240 °C for ethanol and 31 °C for  $\text{CO}_2$ ,<sup>35</sup> as higher temperatures increase the degree of condensation in silica gels.<sup>14</sup> Additionally, condensation within the silica gel produces water, which is much more soluble in ethanol than in  $\text{CO}_2$ . Excess water is more effectively removed from the silica gel by the action of the ethanol solvent, further encouraging condensation within the silicate network.

Drying and annealing were crucial steps in preparing a sample for infiltration. Heating the monolith promoted condensation

(32) Horváth, G.; Kawazoe, K. *J. Chem. Eng. Jpn.* **1983**, *16*, 470–5.

(33) Barrett, E. P.; Joyner, L. G.; Halenda, P. P. *J. Am. Chem. Soc.* **1951**, *73*, 373–80.

(34) *Corning Information Sheet*; Vycor Brand Porous Glass 7930; Corning Inc.: Corning, NY, 2001.

(35) *CRC Handbook of Chemistry and Physics*, 3rd electronic ed. (81st printed ed.); CRC Press: Cleveland, OH, 2000.

(36) Gidley, D. W.; Frieze, W. E.; Dull, T. L.; Yee, A. F.; Ryan, E. T.; Ho, H.-M. *Phys. Rev. B* **1999**, *60*, R5157–60.

(31) Brunauer, S.; Emmett, P. H.; Teller, E. *J. Am. Chem. Soc.* **1938**, *60*, 309–19.

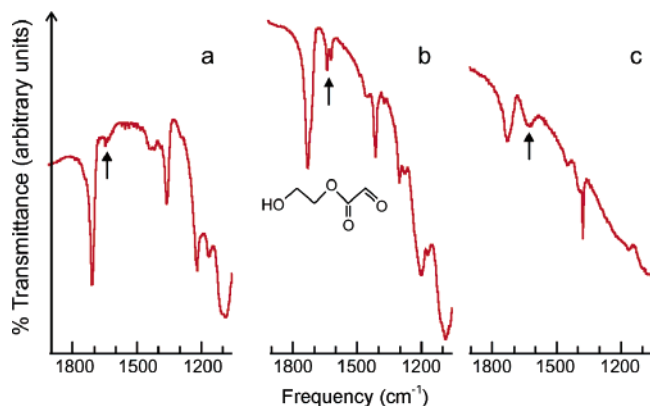


**Figure 5.** Infrared spectra of (a) porous silica before infiltration, (b) silica infiltrated with monomers of hydroxyethyl acrylate, and (c) silica after polymerization. The doublet peak indicated by the arrow in b is attributable to the monomer only and is diminished after polymerization (c).

between neighboring Si—OH groups to form Si—O—Si linkages, thereby strengthening the silica structure, a process aided by heating under dynamic vacuum to remove the products of condensation. Annealing may also relax residual stresses within the channel walls, further strengthening the monolith.

**Infiltration of L<sub>3</sub> Silica by Liquids.** Silica monoliths dried in supercritical ethanol were robust enough to withstand re-infiltration by liquid ethanol and a variety of other organic liquids and solutions. This was an important confirmation of its suitability as a matrix material. One of the significant results of this study is the synthesis of porous silica capable of withstanding the infiltration of liquid following extraction and drying. However, it was found necessary to expose dried monoliths to ethanol vapor prior to introducing the liquid into the channels. The dried samples were not strong enough to withstand capillary stresses caused by the presence of the vapor—liquid boundary at the wetting front of the infiltrating liquid. Pretreatment with ethanol vapor was sufficient to reduce the capillary stresses by wetting the channel surfaces with condensed ethanol. Liquids could then be safely infiltrated into the monolith.

**Photopolymerization.** The optical clarity of the extracted monoliths (Figure 2) was excellent; a representative measurement of the ratio of scattered to transmitted light equaled  $1.5 \times 10^{-6}$  at  $22^\circ$  from the surface normal ( $\sim 0.2$  cm thick disk), equivalent to that of a high-quality glass and superior to samples of infiltrated Vycor.<sup>37</sup>

Polymerization of hydroxyethyl acrylate monomers after infiltration into the silica matrix was done using flood exposure to UV. An initial yellow color was due to the presence of the photoinitiator within the polymer/silica composite and slowly faded over several hours, yielding an optically clear and colorless material. The mid-infrared spectrum of the silica monolith is simply that of silica (Figure 5a). After infiltration, the resulting spectra are still dominated by the silica absorption spectrum (Figure 5b,c). Infiltrating with the hydroxyethyl acrylate monomer is apparent with appearance of the characteristic absorption doublet centered near  $1650\text{ cm}^{-1}$  (Figure 5b). After exposure to UV, this doublet has virtually disappeared, indicating that the monomer has polymerized in situ. A significant aspect of this process was the maintenance of a coherent structure as the silica monolith did not fracture during polymerization.

The samples remained optically clear following polymerization, suggesting that composite optical devices could be made starting

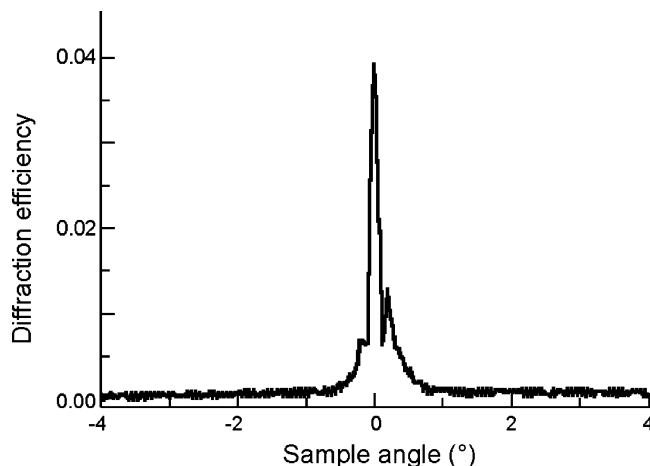


**Figure 6.** Typical Bragg peak obtained from photomonomer-filled L<sub>3</sub> silica. The diffraction strength exhibited does not reflect the maximum refractive index contrast available from the material and could be improved with optimized recording conditions.

from the porous silica and infiltrating photomonomers with desired refractive indices and index changes on photopolymerization. For example, optical paths could be defined by selectively photopolymerizing regions of the infiltrated material. As further evidence that regioselective photochemistry can occur, exposure of a sample infiltrated with photomonomer and photoinitiator to a pair of interfering laser beams produced a grating that gave rise to a diffraction peak (Figure 6). While this grating alone does not constitute firm evidence of information storage capability, it does show that the liquid was fully infiltrated into the bulk of the sample and retained photoactivity after infiltration.<sup>6</sup>

The demonstration that organic monomers can be inserted into our porous silica monoliths, can undergo photopolymerization, and produce a hybrid that retains transparency after both processes opens up a variety of opportunities for fabricating hybrid photonic devices and for producing information storage media. Photonic devices depend first of all on index contrast between cores and claddings in waveguides, between maxima and minima in gratings, and between written and unwritten domains for data recording. In all of these cases, distances and geometries need to be preserved once defined by an initial patterning process; subsequent patterning should not distort the original spatial relationships among domains.

Acrylate polymerizations are compatible with a wide variety of functional groups that confer index contrast, index anisotropy, and index modulation. The ability to perform a high-yield acrylate photopolymerization within the monolith, as judged by infrared spectroscopy (Figure 5), means that these monoliths can be provided with defined bulk refractive index, as well as patterns of refractive index, in a static sense. In addition, dynamic capabilities such as optical shuttering can be conferred, depending on side groups attached to the acrylates. While acrylate polymerizations usually cause significant shrinkage, on the order of 5–10%, the rigid host matrix maintained its dimensions during the conversion to polymer, preventing the distortion that would otherwise accompany polymerization in a soft medium. The polymerization capability is probably not limited to acrylates; other vinyl monomers and even photoacid-induced epoxy polymerizations should be possible.

The maintenance of transparency is of course highly desirable for any photonic application. The ability to produce a grating is suggestive of a holographic storage capability, though is by no means a complete demonstration of data capacity. Rather, it is further evidence that useful photochemistry can be accomplished

(37) Wiltzius, P. Technical Memorandum, Lucent Technologies, 1997.

inside this new porous silicate and that the photopolymerization can be done in a way that forms a usable refractive index pattern.

### Conclusions

We have demonstrated that surfactant-templated, monolithic silica can be supercritically extracted under appropriate solvent to yield a material that resembles an aerogel in its surface area and void volume. But while aerogels are generally quite fragile, the ethanol-extracted L<sub>3</sub> silica structures described herein are sufficiently robust to withstand infiltration by organic liquids. We have demonstrated that infiltration of the silica by an acrylate monomer can be followed by in situ polymerization without damaging the integrity of the monolith, creating an organic/inorganic composite with nanoscale features. Finally, we suggest

that a composite of photomonomer and L<sub>3</sub> silica can be used to successfully write holographic gratings.

**Acknowledgment.** Peter Mirau (Bell Laboratories, Lucent Technologies, Murray Hill, NJ) performed the NMR experiments described above and greatly assisted in the interpretation of the resulting spectra. Lisa Dhar and Melinda Schnoes (Bell Laboratories, Lucent Technologies, Murray Hill, NJ) performed the diffraction studies on photopolymerized composite monoliths. The original support for this research was provided by Lucent Technologies. Support by the NASA University Research, Engineering, and Technology Institute on Bio Inspired Materials (BIMat) under Award NCC-1-02037 is also acknowledged.

LA0514718